Queue Analysis with Finite Buffer by Stochastic Geometry in Downlink Cellular Networks

Qiong Liu, Jean-Yves Baudais, Philippe Mary

▶ **To cite this version:**

Qiong Liu, Jean-Yves Baudais, Philippe Mary. Queue Analysis with Finite Buffer by Stochastic Geometry in Downlink Cellular Networks. 2021 IEEE 93rd Vehicular Technology Conference (VTC2021-Spring), Apr 2021, Helsinki, Finland. pp.1-5, 10.1109/VTC2021-Spring51267.2021.9448646 . hal-03274695

HAL Id: hal-03274695
https://hal.science/hal-03274695

Submitted on 30 Jun 2021

HAL is a multi-disciplinary open access archive for the deposit and dissemination of scientific research documents, whether they are published or not. The documents may come from teaching and research institutions in France or abroad, or from public or private research centers.

L'archive ouverte pluridisciplinaire **HAL**, est destinée au dépôt et à la diffusion de documents scientifiques de niveau recherche, publiés ou non, émanant des établissements d'enseignement et de recherche français ou étrangers, des laboratoires publics ou privés.

Queue Analysis with Finite Buffer by Stochastic Geometry in Downlink Cellular Networks

Qiong Liu*, Jean-Yves Baudais†, Philippe Mary*
*Univ. Rennes, INSA, IETR, Rennes, France
†IETR, CNRS, Rennes, France
Email: qiong.liu@insa-rennes.fr

***Abstract*—In this work, we proposed a tractable mathematical framework to analyze the coverage probability in dynamic downlink cellular networks taking into account the queue dynamics with finite buffer restriction. In particular, the developed model is based on stochastic geometry and queueing theory to handle the interaction between the coverage probability and the queueing state evolution. We also analyze the coverage probability as well as packet loss probability with discrete time Markov chain at stationary regime. We explicitly derive the influence of the packet buffer length to the coverage and packet loss probability. We show in particular that small buffer length leads to a better coverage probability but also to a larger packet loss probability, advocating for a tradeoff between these two metrics.**

***Index Terms*—stochastic geometry, downlink cellular network, instantaneous SINR, DTMC, finite buffer.**

I. Introduction

A. Background and related works

Stochastic geometry provides a mathematical framework to analyze the performance of large scale wireless networks by capturing the spatial randomness intrinsic to the wireless systems including fading, shadowing, and power control [1]–[3]. Recently, stochastic geometry has been combined with more complex network models taking into account frequency reuse, multiple antennas, multiple-tiers or load-aware protocols, to cite a few [4]–[6].

Since real systems are subjected to temporal traffic variations and the sources generate packets according to some stochastic processes [7], the full-load hypothesis, which assumes that each cell uses the same frequency band and is always transmitting, is not enough to address the performance of practical systems. The full load hypothesis generally leads to pessimistic network performance [6].

Therefore, load-awareness is essential for practical performance assessment. The main difficulty is the complex interaction between the packet arrival process and the service rate, which depends on the coverage probability, that depends in turn on the interference distribution over the networks and the dynamic of transmitters' queues. Hence, the distribution of the interferers and the queue length at each transmitter are two interdependent processes which make the analysis of the signal to interference plus noise ratio (SINR) quite challenging [6], [8].

This work has been funded by a China Scholarship Council (CSC) grant.

A simple way to decouple the influence of the interference and the data traffic in the SINR analysis, is to consider that the set of interfering transmitters is a Poisson point process (PPP) randomly thinned from the original PPP according to a certain activity factor [5]–[7]. In [7], authors studied the impact of the activity probability on heterogeneous cellular network performance, e.g. coverage probability, average rate, conditioned on that the typical user connects to the strongest BS. Similarly, [5], [6] integrates stochastic geometry and queueing theory to study sufficient and necessary conditions for queue stability in ad hoc networks. However, the interaction between the queues at different transmitters are either ignored or only analyzed by approximations.

To model the aforementioned interactions between the queues and the interference distribution, authors in [8]–[10] introduced queueing theory in the analysis of the coverage probability. A traffic-aware spatio-temporal model for IoT devices supported by cellular uplink connectivity has been developed in [9]. The authors studied the trade-off between the scalability of the network, i.e. its ability to support a large number of devices, and its stability, i.e. the queues are not diverging. Similarly, a novel spatio-temporal mathematical framework has been developed to analyze the transmission success probability of a cellular network [10], where the number of accumulated packets in the queues is approximated by a Poisson distribution. However, the theoretical findings are not validated by simulations.

To the best of our knowledge, all the works mentioned before studied the coverage probability with infinite queue lengths. However, the packet loss probability is also an important performance measure needed for the design of telecommunication networks. The quantity of interest is the probability of a new packet is dropped when the buffer has a finite size [11], [12]. The main contribution of the paper is to derive the coverage and packet loss probabilities considering the buffer restriction.

B. Approach and contributions

This work proposes a tractable mathematical model to analyze the coverage probability and packet loss probability in a downlink cellular network, in which queue dynamics are taken into consideration. We develop a comprehensive approach to handle the interaction between the coverage probability and the queueing state evolution using a discrete time Markov

chain (DTMC) when a finite buffer length at each transmitter is considered. We derive a closed-form expression of the coverage probability that depends on the fraction of active base stations (BS) that depends in turn to the activity probability which is related to the buffer length. We also characterize the packet loss probability with DTMC the stationary regime.

C. Notations

Throughout the paper, $\mathbb{P}\{\cdot\}$ denotes probability, $\mathbb{E}_X\{\cdot\}$ denotes the expectation over the random variable X. The indicator function is denoted as $\mathbb{1}\{\cdot\}$, which takes values 1 when the statement $\{\cdot\}$ is true and 0 otherwise. The Euclidean norm is denoted as $\|\cdot\|$.

The rest of paper is organized as follows. Section II presents the system model and the assumptions. The coverage and packet loss probabilities are established in Section III. Section IV provides the simulation results and conclusions are drawn in Section V.

II. System model

A. Spatial & physical layer parameters

We consider a single-tier downlink cellular-based network where BSs are spatially distributed in $\mathbb{R}^2$ following an homogeneous PPP $\Phi = \{x_i\}_{i\in\mathbb{N}}$ with intensity λ, where the x_i's are the positions of BS. We assume the user equipments (UEs) density is high enough that every BS has at least one user associated with it. Besides, each UE is served by its nearest BS. A single UE, randomly chosen, is considered as a typical UE and is located at the origin $(0,0)$ for the easy of analysis, with its tagged BS located at x_0. Moreover, every BS is assumed to transmit in the same band, i.e. full frequency reuse.

B. Traffic model

We use a discrete time queueing system to model the random traffic arrival and departure processes. The time is slotted in very short equal intervals. Each time slot can be used for a single transmission attempt, which means that a single packet arrival or departure can take place per time slot.

A geometric inter-arrival packet generation, with parameter $\xi \in [0,1]$ (packet/slot) is assumed at each BS. The arrived packets at each BS are stored in a buffer with finite size until being transmitted successfully. When a packet arrives and the buffer is full, this new arrival packet is dropped. The buffer length restriction B are the same for all BS and is the maximal number of packets the buffer can contained.

Contrarily to the arrival process, the departure process cannot be fixed *a priori*. It is characterized according to the time-dependent SINR distribution. If the received SINR exceeds a predefined threshold θ, the receiver can decode the packet, this packet is transmitted successfully and it can be removed from the queue. If the transmission failed, the packet remains in the buffer and waits for a re-transmission in the next time slot until being successfully transmitted. In this paper, no limit on the number of retransmissions is considered. At each time slot, the transmitters with empty buffer remain silent. Moreover, we define Φ_t as the set of BS that remain active in the time slot $t \in \mathbb{N}$.

The realization of the point process Φ is conditioned on a full time activity of the BS located at x_0. The relevant probability measure over the PPP is then reduced to Palm probability, denoted as $\mathbb{P}^{x_0}$. Correspondingly, the expectation is taken with respect to the measure $\mathbb{P}^{x_0}$.

C. Signal-to-interference ratio

The received SINR at time slot t experienced by the typical UE is

$$\gamma_t = \frac{h_{x_0,t}\left\|x_0\right\|^{-\alpha}}{\sigma^2 + \sum\limits_{x\in\Phi\setminus x_0} h_{x,t}\left\|x\right\|^{-\alpha}\mathbb{1}(x\in\Phi_t)} \tag{1}$$

where $\|x\|$ is the distance between the interfering BS at x and the typical user, $h_{x,t}$ and $h_{x_0,t}$ are the channel gains between the typical UE and the interfering BS at position x and its tagged BS at position x_0 at time slot t, respectively, and they are assumed to be exponentially distributed. α stands for the path loss exponent, σ^2 denotes the power of the additive white Gaussian noise and $\mathbb{1}(x \in \Phi_t)$ indicates whether a node located at $x \in \Phi$ is transmitting at time slot t, i.e. $\mathbb{1}(x \in \Phi_t) = 1$ or not, i.e. $\mathbb{1}(x \in \Phi_t) = 0$. Moreover, we note q_t the quantity

$$q_t = \mathbb{P}_{\mathbb{1}(x\in\Phi_t)}(\mathbb{1}(x \in \Phi_t) = 1) \tag{2}$$

which can be seen as the fraction of active interfering BS at time slot t or equivalently the probability that a randomly chosen BS is active at time slot t.

III. Performance Analysis

The main technical results of the paper are presented now. we first detail the dynamic coverage probability. Then, the traffic analysis and its relation with the coverage probability are performed thanks to a DTMC. By characterizing the stationary regime of this DTMC, we derive the distribution of stable coverage probability and packet loss probability.

A. Dynamic coverage probability

Considering that the typical UE receives data at time slot t, i.e. its associated BS in x_0 is always active, the coverage probability is defined as [6]

$$p_t(\theta,\xi,B) \triangleq \mathbb{P}^{x_0}\left[\gamma_t > \theta\right] \tag{3}$$

where θ is the decoding SINR threshold.

Lemma 1. *The received dynamic coverage probability experience by the typical UE at time t is*

$$p_t(\theta,\xi,B) = 2\pi\lambda\int_0^\infty e^{-\sigma^2\theta r^\alpha} e^{-\pi\lambda r^2(1+q_t\rho(\alpha,\theta))} r\mathrm{d}r \tag{4}$$

where $\rho(\alpha,\theta) = \int_1^\infty [1+u^{\frac{\alpha}{2}}\theta^{-1}]^{-1}du$.

Proof. See Appendix A. □

Lemma 1 quantifies how the coverage probability behaves at a given time slot and depends on the traffic. The queue

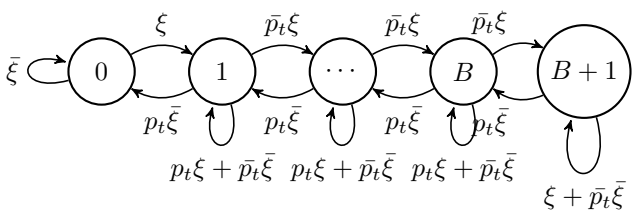

Figure 1. DTMC model.

states are affecting the coverage probability via the parameter q_t. As q_t decreases, less interferers are actives in the network, and hence, the aggregate interference decreases and dynamic coverage probability increases at typical BS.

To characterize q_t, a Markov chain with $B+2$ states is considered where the state space is $\{0, 1, \cdots, B, B+1\}$ as illustrated in Fig. 1. State 0 represents the empty buffer event. When the buffer is in this state, the transmitter remains silent. When the queue is in state B, it means the buffer is full and hence any new generated packet is dropped, i.e. state $B+1$. Since the packets arrive according to the Bernoulli process with parameter ξ and the service is then geometric with parameter p_t, the number of packets at an arbitrary time instant can be modeled as the DTMC given in Fig. 1. Note that q_t is the complementary probability for the queue to be in state 0 at each time slot.

B. Stable coverage probability

The network is called stable if the number of active transmitters converges regardless of the network initial condition [13]. Let $\widetilde{\Phi}$ be the limit of Φ_t as $t \to \infty$, which represents the point process in the stable regime. Let $q = \mathbb{P}_{\mathbb{1}(x\in\widetilde{\Phi})}(\mathbb{1}(x \in \widetilde{\Phi}) = 1)$. The stable coverage probability is defined as

$$p(\theta, \xi, B) = \lim_{t\to\infty} p_t(\theta, \xi, B) \tag{5}$$

Lemma 2. *Considering $q_{t\to\infty} = q$, the stable coverage probability is*

$$p(\theta, \xi, B) = 2\pi\lambda \int_0^\infty e^{-\sigma^2\theta r^\alpha} e^{-\pi\lambda r^2(1+q\rho(\alpha,\theta))} r \mathrm{d}r \tag{6}$$

where $\rho(\alpha, \theta) = \int_1^\infty [1 + u^{\frac{\alpha}{2}}\theta^{-1}]^{-1} du$.

Proof. See Appendix B. □

By characterizing the stationary regime of DTMC, we decouple the time dependence of the coverage probability and the queue states. Thanks to Lemmas 1 and 2, we are now ready to present our main result of this paper, i.e. the stable coverage probability with finite buffer restriction.

Theorem 1. *The stable coverage probability with a finite buffer restriction B is given by the fix point equation*

$$p(\theta, \xi, B) \tag{7}$$
$$= 2\pi\lambda \int_0^\infty e^{-\sigma^2\theta r^\alpha} e^{-\pi\lambda r^2 \left(1+\frac{(R^{B+2}-R)\rho(\alpha,\theta)}{R^{B+2}-R+(R-1)\bar{p}(\theta,\xi,B)}\right)} r \mathrm{d}r$$

where $\bar{p}(\theta, \xi, B) = 1 - p(\theta, \xi, B)$, and $R = \frac{\xi\bar{p}(\theta,\xi,B)}{\bar{\xi}p(\theta,\xi,B)}$.

Proof. See Appendix C. □

Corollary 1. *In an interference-limited network, i.e. $\sigma^2 \to 0$, we have*

$$p(\theta, \xi, B) = \left[1 + \Upsilon \int_1^\infty \frac{1}{1 + u^{\frac{\alpha}{2}}\theta^{-1}} du\right]^{-1} \tag{8}$$

where $\Upsilon = 1 + (1 - R^{B+2})^{-1}(1 - R)^{-1}(1 - p(\theta, \xi, B))$. When the path loss exponent $\alpha = 4$, the stable coverage probability can be further simplified to

$$p(\theta, \xi, B) = \left[1 + \Upsilon\sqrt{\theta}(\frac{\pi}{2} - \arctan\sqrt{\theta})\right]^{-1} \tag{9}$$

For the sake of simplicity, we use p instead of $p(\theta, \xi, B)$ in the rest of this paper. The fix point equation expressed in Theorem 1 can be iteratively solved using Algorithm 1.

Algorithm 1 Iteration algorithm for computation of p and q.

```
Initialize q_1 ∈ (ξ, 1), q_0 = 0, i = 0, ε ≪ 1
while |q_{i+1} − q_i| ≥ ε do
  i ← i + 1, q ← q_i, p ← p (22) in Appendix C
  if |q_{i+1} − q_i| ≥ ε then
    q_{i+1} ← q (21) in Appendix C
    break
  end if
end while
Return q ← q_{i+1} and p
```

C. Packet loss probability

The packet loss probability is the probability that a new packet is dropped when it meets the maximum queue length situation and is given by the following lemma.

Lemma 3. *The packet loss probability at a randomly chosen BS with finite buffer length restriction B is given by*

$$p_{loss} = \frac{R^{B+2} - R^{B+1}}{(R-1)\bar{p} + R^{B+2} - R} \tag{10}$$

where p is the stable coverage probability in Theorem 1 and $R = \frac{\xi\bar{p}}{\bar{\xi}p}$.

Proof. p_{loss} is the probability to be in the state $B+1$. According to (16) and Theorem 1, the result is obtained after some algebraic manipulations. □

IV. Numerical results and simulations

BS positions are generated using a PPP with density $\lambda = 0.25$. Each UE is associated to its nearest BS. The packets arrive to each BS according to the Bernoulli process with parameter ξ and the service is then geometric with parameter p_t at each time slot. For each network realization, the queues are let to evolve up to the convergence, i.e. the number of active transmitters does not evolve with time, then a new network realization is drawn and the process repeats.

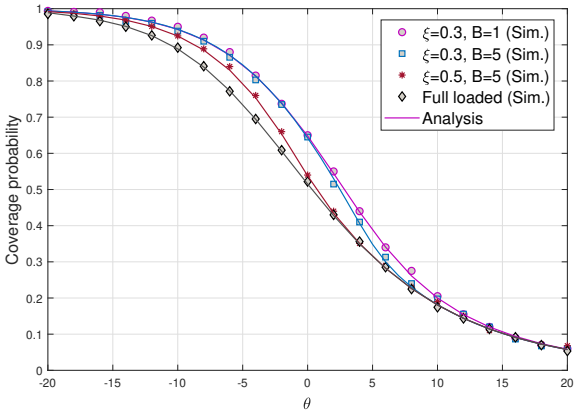

Figure 2. Coverage probability at stable state with different buffer restrictions B and arrival rates ξ.

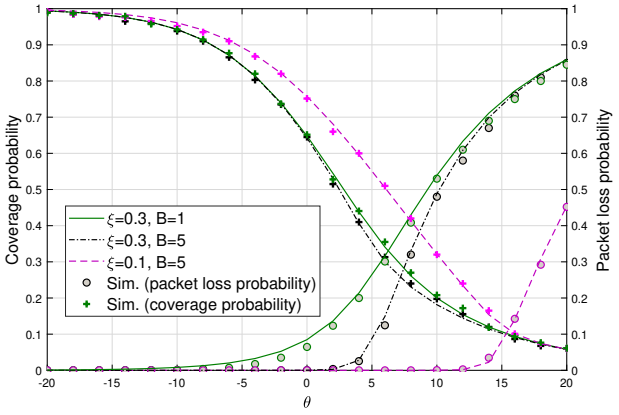

Figure 3. Packet loss probability and coverage probability at stable state ($\lambda = 0.25$, $\sigma^2 = -10$ dB, $\alpha = 4$).

Fig. 2 compares the analytical result obtained in Theorem 1 evaluated with Algorithm 1, with the Monte-Carlo simulations under different arrival rate ξ as well as different buffer restriction B. First, we observe that the full load model is pessimistic w.r.t. the coverage probability. When the buffer length is kept constant, e.g. $B = 5$, we observe that the higher the arrival rate, the lower the coverage probability, on a large range of coverage threshold θ. Indeed, when ξ increases the queues are more solicited and hence BSs often have a packet to transmit and hence they generate interference. A more surprising result, is the dependency of the coverage probability with the buffer size when the arrival rate is fixed, i.e. $\xi = 0.3$. We notice that when the buffer length increases, i.e. B changes from 1 to 5, the coverage probability degrades for thresholds between 2 dB and 14 dB. This is due to the fact that BS with a large B drop less packets than BS with a smaller queue size, for a given arrival rate. Hence, the activity probability is larger when $B = 5$ than when $B = 1$ that increases the interference and hence decreases the coverage probability. However, a very constraint queue size implies an important packet loss since the probability that a randomly chosen queue be full is higher when $B = 1$ than when $B = 5$.

Fig. 3 plots the coverage probability and the packet loss probability in Lemma 3 w.r.t the threshold θ, and labeled on the arrival rate ξ and the queue length B. When fixing the queue length $B = 5$, we observe that the coverage probability improves when the arrival rate decreases, i.e. from $\xi = 0.3$ to $\xi = 0.1$ since the network generates less packets in the second case and hence the probability for a BS to be idle increases, that decreases the interference to the typical user. Moreover, since less packets are generated the packet loss probability also decreases for a given coverage threshold. When fixing the arrival rate $\xi = 0.3$, we observe that the packet loss decreases significantly when B increases for low to medium range of values of θ.

V. Conclusion

In this paper, we proposed a tractable mathematical model to analyze the stable coverage probability and packet loss probability in a dynamic traffic randomly deployed downlink cellular network with finite buffer length. The queue evolution at each transmitter has been handled with a DTMC and a Bernoulli distribution for packet arrival. The interaction between the coverage probability and the queue state evolution has been captured in closed-form. We also discussed the impact of different arrival rates and different buffer lengths to the network performance, measured with the coverage probability and the packet loss probability.

Appendix

A. Proof of Lemma 1

Given the typical UE received data at time slot t, its conditional SINR coverage probability is written as (to lighten the notation we remove the index t from the channel coefficients)

$$
\begin{aligned}
p_t &= \mathbb{P}^{x_0}(\gamma_t \geq \theta) \\
&= \mathbb{P}^{x_0}\left[\frac{h_{x_0}\left\|x_0\right\|^{-\alpha}}{\sigma^2 + \sum\limits_{x\in\Phi\setminus x_0} h_x \left\|x\right\|^{-\alpha} \mathbb{1}(x \in \Phi_t)} \geq \theta\right] \\
&= \int_0^\infty 2\pi\lambda r_0 e^{-\pi\lambda r_0^2} \exp(-\sigma^2\theta r_0^\alpha) \\
&\quad \times \mathbb{P}^{x_0}\left[\frac{h_{x_0}\left\|x_0\right\|^{-\alpha}}{\sigma^2 + \sum\limits_{x\in\Phi\setminus x_0} h_x \left\|x\right\|^{-\alpha} \mathbb{1}(x \in \Phi_t)} \geq \theta \middle| \|x_0\| = r_0\right] \mathrm{d}r_0 \\
&= \int_0^\infty 2\pi\lambda r_0 e^{-\pi\lambda r_0^2} e^{-\sigma^2\theta r_0^\alpha} \mathcal{L}_I(\theta r_0^\alpha) \mathrm{d}r_0 \qquad (11)
\end{aligned}
$$

where the Laplace transform (LT) of a random variable X in s is denoted as $\mathcal{L}_X(s)$. Further, the LT $\mathcal{L}_X(s)$ in (11), with

$s=\theta r_0^{\alpha}$, has the form:

$$\begin{aligned}
\mathcal{L}_I(s) &= \mathbb{E}\Big[\exp\Big(-s\sum_{x\in\Phi\setminus x_0} h_x \left\|x\right\|^{-\alpha}\mathbb{1}(x\in\Phi_t)\Big)\Big|r_0\Big] \\
&\overset{a}{=} \mathbb{E}_{\Phi}\left[\prod_{x\in\Phi\setminus x_0}\mathbb{E}_{h_x}\Big[\exp\Big(-sh_x\left\|x\right\|^{-\alpha}\mathbb{1}(x\in\Phi_t)\Big)\Big]\Big|r_0\right] \\
&= \mathbb{E}_{\Phi}\left[\prod_{x\in\Phi\setminus x_0}\frac{1}{1+s\left\|x\right\|^{-\alpha}\mathbb{1}(x\in\Phi_t)}\Big|r_0\right] \\
&= \mathbb{E}_{\{\mathbb{1}(x\in\Phi_t)\}}\left(\mathbb{E}_{\Phi}\left[\prod_{x\in\Phi\setminus x_0}\frac{1}{1+s\left\|x\right\|^{-\alpha}\mathbb{1}(x\in\Phi_t)}\Big|\begin{matrix}r_0,\\ \mathbb{1}(x\in\Phi_t)\end{matrix}\right]\right) \\
&\overset{b}{=} \mathbb{E}_{\Phi}\left[\prod_{x\in\Phi\setminus x_0}\left(\frac{\mathbb{E}_{\mathbb{1}(x\in\Phi_t)}[\mathbb{1}(x\in\Phi_t)=1]}{1+s\left\|x\right\|^{-\alpha}\times 1}\right.\right. \\
&\qquad \left.\left.+\frac{\mathbb{E}_{\mathbb{1}(x\in\Phi_t)}[\mathbb{1}(x\in\Phi_t)=0]}{1+s\left\|x\right\|^{-\alpha}\times 0}\right)\Big|r_0\right] \\
&\overset{c}{=} \mathbb{E}_{\Phi}\left[\prod_{x\in\Phi\setminus x_0}\left(\frac{q_t}{1+s\left\|x\right\|^{-\alpha}}+1-q_t\right)\Big|r_0\right] \qquad (12)
\end{aligned}$$

where (a) follows from the i.i.d. hypothesis of h_x and further independence from the point process Φ, (b) follows from the law of total expectation and using independence activity of BS [9, Assumption 2], and (c) follows from $q_t=\mathbb{P}(\mathbb{1}(x\in\Phi_t)=1)$.

According to the PGFL of PPP and with $r=\left\|x\right\|$, we have

$$\begin{aligned}
&\mathcal{L}_I(\theta r_0^{\alpha}) \\
&= \exp\left(-2\pi\lambda\int_{r_0}^{\infty}\left(1-\left(\frac{q_t}{1+\theta r_0^{\alpha}r^{-\alpha}}+1-q_t\right)\right)r\mathrm{d}r\right) \\
&\overset{a}{=} \exp\left(-\pi\lambda r_0^2\int_1^{\infty}\frac{q_t}{1+u^{\frac{\alpha}{2}}\theta^{-1}}\mathrm{d}u\right) \qquad (13)
\end{aligned}$$

where (a) is obtained by the change of variable $u=(\frac{r}{r_0})^2$.

B. Proof of Lemma 2

Considering $q_{t\to\infty}=q$, we have

$$\begin{aligned}
p &= \lim_{t\to\infty} p_t(\theta,\xi,B) \\
&= \lim_{t\to\infty} 2\pi\lambda\int_0^{\infty} e^{-\sigma^2\theta r^{\alpha}}e^{-\pi\lambda r^2(1+q_t\rho(\alpha,\theta))}r\mathrm{d}r \\
&\overset{a}{=} 2\pi\lambda\int_0^{\infty} e^{-\sigma^2\theta r^{\alpha}}e^{-\pi\lambda r^2\left(1+q_{\lim_{t\to\infty}}\rho(\alpha,\theta)\right)}r\mathrm{d}r \\
&= 2\pi\lambda\int_0^{\infty} e^{-\sigma^2\theta r^{\alpha}}e^{-\pi\lambda r^2(1+q\rho(\alpha,\theta))}r\mathrm{d}r \qquad (14)
\end{aligned}$$

where $\rho(\alpha,\theta)=\int_1^{\infty}[1+u^{\frac{\alpha}{2}}\theta^{-1}]^{-1}du$. (a) follows the fact that p_t is non-negative and continuous. Let $A(r)=e^{e^{-\sigma^2\theta r^2}}$, and $g=A(r)e^{-\pi\lambda r^2}$, we have $\left|A(r)e^{-\pi\lambda(1+q_t\rho(\alpha,\theta))}\right|\le g,\ \forall\theta>0, t\in\mathbb{N}$. Since g is integrable, by the dominant convergence theorem, we have p and the result follows.

C. Proof of Theorem 1

The number of packets in the queue can be characterized by the stationary distribution of DTMC in Fig. 1. When $t\to\infty, q=\mathbb{P}_{\mathbb{1}(x\in\widetilde{\Phi})}(\mathbb{1}(x\in\widetilde{\Phi})=1)$, p is given in (14). The transition probability matrix writes

$$\mathbf{P}=\begin{bmatrix}
\bar{\xi} & \xi & 0 & 0 & \cdots & 0 \\
p\bar{\xi} & \bar{p}\bar{\xi}+p\xi & \bar{p}\xi & 0 & \cdots & 0 \\
0 & p\bar{\xi} & \bar{p}\bar{\xi}+p\xi & \bar{p}\xi & \cdots & 0 \\
0 & 0 & \ddots & \ddots & \ddots & 0 \\
0 & 0 & 0 & p\bar{\xi} & \bar{p}\bar{\xi}+p\xi & \bar{p}\xi \\
0 & 0 & 0 & 0 & p\bar{\xi} & \bar{p}\bar{\xi}+\xi
\end{bmatrix} \qquad (15)$$

For stationary Markov chains, we have

$$\boldsymbol{\pi}\mathbf{P}=\boldsymbol{\pi},\ \boldsymbol{\pi}\boldsymbol{e}=1 \qquad (16)$$

where $\boldsymbol{\pi}=[\pi_0,\pi_1,\pi_2,\cdots,\pi_B,\pi_{B+1}]$ is the row vector that contains the stationary probabilities, in which $\pi_i(1\le i\le B)$ denotes the probability of being in state with i packets, π_{B+1} denotes the probability of a new packet is dropped when it meets the maximum queue length situation, and $\boldsymbol{e}$ is a column vector of ones with the proper length.

The solution of (16) is the solution of

$$\begin{cases}
\pi_0=\pi_0\bar{\xi}+\pi_1\bar{\xi}p \\
\pi_1=x_0\xi+\pi_1(\bar{\xi}\bar{p}+p\xi)+x_2\bar{\xi}p \\
\pi_i=\pi_{i-1}\xi\bar{p}+x_i(\bar{\xi}\bar{p}+p\xi)+\pi_{i+1}\bar{\xi}p,\ 2\le i\le B \\
\pi_{B+1}=\pi_B\xi\bar{p}+\pi_{B+1}(\bar{p}+p\xi)
\end{cases} \qquad (17)$$

according to (17), we have

$$\pi_i=\frac{\pi_0}{\bar{p}}(\frac{\xi\bar{p}}{\bar{\xi}p})^i,\quad 1\le i\le B \qquad (18)$$

$$\pi_{B+1}=(\frac{\xi\bar{p}}{\bar{\xi}p})^B\frac{\xi}{\bar{\xi}p}\pi_0 \qquad (19)$$

After normalization, we obtain

$$\pi_0=\left[1+\xi R^B(\bar{\xi}p)^{-1}+(\bar{p})^{-1}\sum_{i=1}^{B}R^i\right]^{-1} \qquad (20)$$

where $R=\frac{\xi\bar{p}}{\bar{\xi}p}$. Combine (20) and (14), and the condition that $q=1-\pi_0$, we have

$$q=1-\left[1+\xi R^B(\bar{\xi}p)^{-1}+\sum_{i=1}^{B}R^i(\bar{p})^{-1}\right]^{-1} \qquad (21)$$

$$p=2\pi\lambda\int_0^{\infty}e^{-\sigma^2\theta r^{\alpha}}e^{-\pi\lambda r^2(1+q\rho(\alpha,\theta))}r\mathrm{d}r \qquad (22)$$

where $\bar{a}=1-a$ with $a\in\{p,\xi\}$, $\rho(\alpha,\theta)=\int_1^{\infty}[1+u^{\frac{\alpha}{2}}\theta^{-1}]^{-1}du$, $R=\frac{\xi\bar{p}}{\bar{\xi}p}$. According to (21) and (22), the inter-dependence between q and p shows the relationship between the queue and the stochastic geometry in the analysis. After some manipulations, we obtain the result.

REFERENCES

[1] J. G. Andrews, F. Baccelli, and R. K. Ganti, "A tractable approach to coverage and rate in cellular networks," *IEEE Transactions on Communications*, vol. 59, no. 11, pp. 3122–3134, 2011.

[2] H. Elsawy and E. Hossain, "On stochastic geometry modeling of cellular uplink transmission with truncated channel inversion power control," *IEEE Transactions on Wireless Communications*, vol. 13, no. 8, pp. 4454–4469, 2014.

[3] T. D. Novlan, H. S. Dhillon, and J. G. Andrews, "Analytical modeling of uplink cellular networks," *IEEE Transactions on Wireless Communications*, vol. 12, no. 6, pp. 2669–2679, 2013.

[4] H. ElSawy, A. Sultan-Salem, M. S. Alouini, and M. Z. Win, "Modeling and Analysis of Cellular Networks Using Stochastic Geometry: A Tutorial," *IEEE Communications Surveys and Tutorials*, vol. 19, no. 1, pp. 167–203, 2017.

[5] Y. Zhong, T. Q. Quek, and X. Ge, "Heterogeneous cellular networks with spatio-temporal traffic: Delay analysis and scheduling," *IEEE Journal on Selected Areas in Communications*, vol. 35, no. 6, pp. 1373–1386, 2017.

[6] Y. Zhong, M. Haenggi, T. Q. Quek, and W. Zhang, "On the stability of static poisson networks under random access," *IEEE Transactions on Communications*, vol. 64, no. 7, pp. 2985–2998, 2016.

[7] H. S. Dhillon, R. K. Ganti, and J. G. Andrews, "Load-aware modeling and analysis of heterogeneous cellular networks," *IEEE Transactions on Wireless Communications*, vol. 12, no. 4, pp. 1666–1677, 2013.

[8] H. H. Yang and T. Q. S. Quek, "Spatio-temporal analysis for sinr coverage in small cell networks," *IEEE Transactions on Communications*, vol. 67, no. 8, pp. 5520–5531, 2019.

[9] M. Gharbieh, H. Elsawy, A. Bader, and M. S. Alouini, "Spatiotemporal Stochastic Modeling of IoT Enabled Cellular Networks: Scalability and Stability Analysis," *IEEE Transactions on Communications*, vol. 65, no. 8, pp. 3585–3600, 2017.

[10] N. Jiang, Y. Deng, X. Kang, and A. Nallanathan, "Random access analysis for massive IoT networks under a new spatio-temporal model: A stochastic geometry approach," *IEEE Transactions on Communications*, vol. 66, no. 11, pp. 5788–5803, 2018.

[11] A. S. Alfa, *Applied Discrete-Time Queues*. New York, NY, USA: Springer, 2016.

[12] W. Ni, J. A. Zhang, Z. Fang, M. Abolhasan, R. P. Liu, and Y. J. Guo, "Analysis of finite buffer in two-way relay: A queueing theoretic point of view," *IEEE Transactions on Vehicular Technology*, vol. 67, no. 4, pp. 3690–3694, 2018.

[13] A. AlAmmouri, J. G. Andrews, and F. Baccelli, "Stability and metastability of traffic dynamics in uplink random access networks," *preprint arXiv:1906.04683*, 2019.